UWB Impulse Radar for Vital Signs Sensing - A Modeling Framework for Arbitrary Periodic Heart and Lung Motion

Van Nguyen and Mary Ann Weitnauer*
School of Electrical and Computer Engineering, Georgia Institute of Technology, Atlanta, GA, 30332-0250
Email: vannguyen@gatech.edu, maweit@gatech.edu

***Abstract*—The Impulse Radio Ultra-wideband (IR-UWB) vital signs application is typically characterized by a periodic transmitted waveform and a periodic delay modulation caused by periodic chest displacement. We present closed-form spectral coefficients for the chest-reflected IR-UWB signal as it arrives at the radar receiver, assuming a planar chest model. We assume the chest displaces according to arbitrary periodic motion of the heart and lungs. Our base model assumes a periodic train of transmitted impulses. We call our approach a "framework" because our model can be put with any burst waveform that is transmitted periodically (such as a pseudo-random binary sequence), any multi-layer model of the chest, and any receiver signal processing model, to provide a complete model of the post-processed radar received signal. We describe in the paper how each of these extensions can be done in a straightforward way with our model, without having to re-derive the coefficients of the base model. Our model is more general than existing models, which lack closed form expressions or have various constraints, such as sinusoidal chest displacement, zero phase, or unavoidable aliasing.**

I. Introduction

The use of Impuse Radio Ultra-wideband (IR-UWB) has been recommended by many researchers for continuous, non-contact vital signs monitoring [1]–[7]. Thanks to its ability to penetrate through obstacles and its excellent spatial resolution, IR-UWB radar can sense, in a *non-contact* manner, the minute chest displacements induced by lungs breathing and heart beating and thereby enable estimation of heart rate (HR) and respiration rate (RR) [1]–[7]. The IR-UWB system emits an extremely low power, non-ionizing signal, which makes negligible interference on co-existing radio systems, and is very robust to multipath and interference [8]. Thus IR-UWB radar is suitable in settings from home health care, hospitals, to rescue operation.

This paper analyzes the signal received by the IR-UWB radar vital signs sensor, which can be located in proximity to the patient, such as under a mattress or behind a chair. An IR-UWB system transmits a series of pulses of duration on the order of a nanosecond. These pulses reflect from boundaries between materials with different dielectric properties, such as the air-skin interface. The time a reflected pulse arrives at the receiver is determined by the round trip distance between the IR-UWB system and the boundary reflecting the pulse. Breathing and heart beating causes the chest interface to move, thereby modulating the round-trip distance; hence the radar received signal is delay-modulated.

We present the first complete analytical framework of the spectral characteristics of the IR-UWB radar received signal for an arbitrary periodic chest displacement model. The received signal is assumed to contain only the reflection from the air-skin interface, modeled as an infinite plane. Although the human thorax tissues have many layers [9], composed of, e.g., skin, fat, muscle, cartilage, lung, heart, and blood, we consider only reflection from the skin layer, because most of the reflected energy is from the skin-air interface, rather than from the interfaces inside the body. For example, at 5 GHz, reflected energy from lung and reflected energy from heart are 87 dB and 130 dB below that from skin, respectively [9]. An example plot of the post down-conversion spectrum produced by our model versus the baseband frequency Δf is shown in Fig. 1. The RR fundamental component (f_b) and its harmonics ($2f_b, 3f_b$), the HR fundamental (f_h), and some intermodulation products (*intermods*), e.g., $f_b + f_h$, are clearly observed. The analysis can be readily extended to the case where reflections come from multiple body tissue layers, such as lung walls and heart wall through superposition. Also, our model can be used with any periodic transmitted waveform, such as pseudo-random sequences that are periodically transmitted [10]. Our model captures the signal as it arrives at the receiver and therefore it can be used to analyze any receiver signal processing scheme, such as multi-pulse integration to improve the signal-to-noise ratio, by integrating our model with a model of the receiver. In other words, our delay-modulated signal model is a critical core component that enables a full system model.

The chest displacement is assumed to consist of the periodic breathing-induced displacement and the periodic heartbeat-induced displacement, but there is no restriction on the respiration phase and heart beating phase at signal acquisition time. In other words, the starting times of the heart beat cycle and the respiration cycle are arbitrary. In our model, the coefficient and frequency of each spectral component have a closed-form.

Our proposed model should have several uses. Signal models are essential in the development of signal processing techniques. Spectral analysis is a common approach for radar-based vital signs estimation, but typical estimation schemes focus only on the frequency locations of spectral peaks as a

*Mary Ann Weitnauer was formerly Mary Ann Ingram.

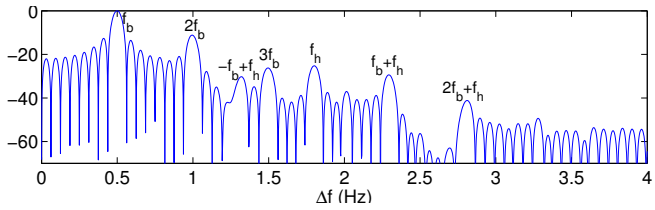

Fig. 1. An example of a radar received spectrum obtained with our model.

means of estimating rates [2]–[6] and ignore peak heights. In contrast, our model will allow investigation into how breathing and heart *patterns* of movement impact the shape of the IR-UWB spectrum. For example, our findings show how the heights of the spectral peaks in the received spectrum depend on the maximum chest displacement; we note this is not a trivial dependence in delay modulation, which is a nonlinear modulation. Furthermore, with the growing interest in modeling breathing and heart beating activities, which affect the chest displacement, the model may help researchers use IR-UWB measurements to validate their lung and heart motion models.

II. Related work

The spectrum of the IR-UWB radar received signal has been derived for several specific displacement models. The theoretical analysis in [5], with the chest displacement assumed to be solely due to breathing and modeled as a sinusoid of the RR fundamental (f_b), shows that the IR-UWB radar signal contain the RR fundamental and its harmonics. Mabrouk *et al* [7] expand this analytical framework by modeling the pulse-reflecting surface as the sum of both chest and abdomen movements, where the chest movement is modeled as a sinusoid of f_b and the abdomen movement is composed of a sinusoid at f_b and another at the second harmonic ($2f_b$), resulting in a spectrum model that contains spectral components also at multiples of RR. Lazaro [6] expands the analysis in [5] by also incorporating the heart beating into the overall chest displacement; the chest displacement is modeled as the sum of a sinusoid of f_b and another sinusoid of the HR fundamental. The resulting spectrum model contains spectral components at multiples of RR, multiples of HR, and their intermods.

However, these displacement models are rather restrictive. First, the sinusoid is not an adequate model for normal breathing displacement because empirically, a person spends more time on exhalation than inhalation in a breathing cycle [11], [12]. In addition, heart beating is a relatively bursty activity that is far from a sinusoidal behavior [13], [14]. Second, in [5]–[7] the sinusoidal displacements are all assumed to start with zero phase. In reality, there is no guarantee that the breathing phase is zero and the relative phase of the heart beating and respiration is zero at data aquisition time.

Three additional points can be made about the existing IR-UWB received spectrum models [5]–[7]. First, the derived spectrum expressions are obtained based on computing the Fourier transform of an undersampled or aliased version of the radar received signal. The spectral components of the aliased spectrum are different from those of the spectrum of the unsampled signal, and generally aliasing is not invertible and some information is lost [15]. In contrast, our model provides the spectrum of the analog signal, i.e., before sampling. Second, one generally has to re-derive the expressions when a new pulse delay model is of interest. Our model, on the other hand, has final expressions that can be easily modified to accommodate changes such as changes in phase. Lastly, the coefficients of the spectral components in [5]–[7] do not have closed form expressions, in general, whereas our model's coefficients have closed forms.

This paper is organized as follows. Section III presents our analytical model of the radar received signal spectrum for the general chest displacement model. Since our signal model is complete and un-aliased, we are able to derive from it the aliased spectrum, and show how they are different, as we do in Section IV. Section V concludes the work.

III. Derivation of the model

The received signal is assumed to contain only the reflection from the air-skin interface, modeled as an infinite plane [1]. The periodic chest displacement can be expressed as a summation of a periodic breathing-induced displacement and a periodic heartbeat-induced displacement, each of which is represented by a Fourier series expansion. Mathematically, the round-trip propagation delay caused by chest displacement of an UWB pulse can be modeled as

$$\begin{aligned}\tau_d(t) = A_0 &+ \sum_{p=1}^{N_b} \left[B_p^b \sin 2\pi(pf_b)t + A_p^b \cos 2\pi(pf_b)t\right] \\ &+ \sum_{q=1}^{N_h} \left[B_q^h \sin 2\pi(qf_h)t + A_q^h \cos 2\pi(qf_h)t\right], \quad (1)\end{aligned}$$

where f_b is the respiration rate [Hz], f_h is the heart rate [Hz], N_b and N_h are the numbers of non-DC Fourier series coefficients of the breathing-induced delay and the heartbeat-induced delay, respectively. A_0 combines the DC components of the breathing-induced and heartbeat-induced delays and the delay due to the nominal distance between the radar and the patient's chest. Note that there is no assumption on the phase of the breathing-induced delay and the phase of the heartbeat-induced delay; they are incorporated in the Fourier series coefficients $\{B_p^b, A_p^b, B_q^h, A_q^h : p = 1, \ldots, N_b; q = 1, \ldots, N_h\}$.

The IR-UWB radar system transmits pulses or short bursts with the repetition period of T_r. Assuming the chest location can be assumed constant for the duration of the pulse or burst, the round-trip delay of the n-th pulse or burst can be represented as the n-th sample of $\tau_d(t)$ with the time sampling

[1] As in [5]–[7], we assume that the environment is static so the only motion that modulates the radar signal is from the movement induced by breathing and heart beating. Each recorded waveform is a superposition of a pulse reflected from the moving chest and pulses reflected from the static clutter. A "motion filter" [5], [6] suppresses the static clutter-reflected pulses but retains the moving-chest-reflected pulses.

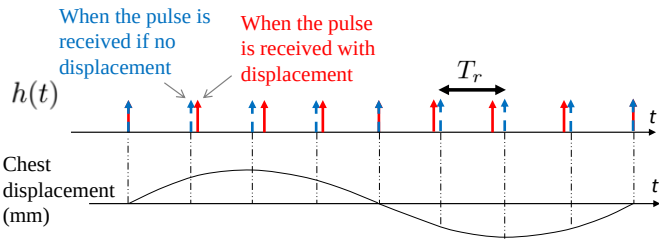

Fig. 2. The channel response of the physiological sensing IR-UWB radar system to a series of impulses for sine chest displacement.

interval equal to T_r: $\tau_{d,n} = \tau_d(nT_r)$, where $\tau_d(t)$ is given in (1).

The propagation effects on the transmitted waveform as it travels from the radar transmitter to the radar receiver can be modeled as a time-varying linear channel. Assuming the planar chest model and and motion filtering to reject static clutter, the only necessary channel effect is one time-varying delay, so the impulse response is simply a delayed Dirac delta function such that the delay is a periodic function of time. Constant amplitude reductions, e.g. due to path loss, are ignored, since they would have the effect of simply scaling the received signal spectrum. We start by assuming that the UWB system emits perfect impulses and that the observation window is of infinite length; these assumptions are removed later. The channel response to a periodic train of impulses with period T_r, is $h(t) = \sum_{n=-\infty}^{\infty} \delta(t - nT_r - \tau_{d,n})$ and is illustrated in Fig. 2 for the chest displacement modeled as a sine waveform. The continuous time Fourier transform (CTFT) of $h(t)$ is $H(f) = \sum_{n=-\infty}^{\infty} e^{-j2\pi f(nT_r+\tau_{d,n})}$ and is derived to be

$$H(f) = \sum_{i}\sum_{k_1}\cdots\sum_{k_{N_b}}\sum_{k'_1}\cdots\sum_{k'_{N_b}}\sum_{l_1}\cdots\sum_{l_{N_h}}\sum_{l'_1}\cdots\sum_{l'_{N_h}} c(f_{\mathbf{z}})\delta\Big(f - f_{\mathbf{z}}\Big), \quad (2)$$

where $\mathbf{z} = [k_1, \ldots, k_{N_b}, k'_1, \ldots, k'_{N_b}, l_1, \ldots, l_{N_h}, l'_1, \ldots, l'_{N_h}, i]$, $f_{\mathbf{z}} = [\sum_{p=1}^{N_b} p(k_p + k'_p)]f_b + [\sum_{q=1}^{N_h} q(l_q + l'_q)]f_h + if_r$, and

$$c(f) = f_r \times (-1)^{\sum_{p=1}^{N_b} k_p + \sum_{q=1}^{N_h} l_q} \times (-j)^{\sum_{p'=1}^{N_b} k'_{p'} + \sum_{q'=1}^{N_h} l'_{q'}} \times \prod_{p=1}^{N_b} J_{k_p}(2\pi B^b_p f) \prod_{p'=1}^{N_b} J_{k'_{p'}}(2\pi A^b_{p'} f) \times \prod_{q=1}^{N_h} J_{l_q}(2\pi B^h_q f) \prod_{q'=1}^{N_h} J_{l'_{q'}}(2\pi A^h_{q'} f) \times e^{-j2\pi A_0 f},$$

where $f_r = 1/T_r$ is the impulse repetition frequency.

Sketch of proof: To reduce complexity, assume the DC component in (1) is zero, i.e., $A_0 = 0$. When $A_0 \neq 0$, the resulting expression will be simply multiplied by $e^{-j2\pi A_0 f}$. Denote $\Omega = 2\pi f, \Omega_b = 2\pi f_b, \Omega_h = 2\pi f_h$. We begin with $H(f) = \sum_{n=-\infty}^{\infty} e^{-j\Omega nT_r} e^{-j\Omega\tau_{d,n}}$. Into $e^{-j\Omega\tau_{d,n}}$, we substitute $\tau_{d,n} = \tau_d(nT_r)$ using (1), and apply the property $\exp\{\sum_k \alpha_k\} = \prod_k \exp\{\alpha_k\}$ to get a product with four factors of similar form; two of them are $\prod_{p=1}^{N_b} \exp\{-j\Omega B^b_p \sin p\Omega_b nT_r\}$ and $\prod_{q'=1}^{N_h} \exp\{-j\Omega A^h_{q'} \cos q'\Omega_h nT_r\}$. Each exponential term is then expanded as a power series using the Jacobi–Anger expansion $e^{jz\sin\theta} = \sum_{n=-\infty}^{\infty} J_n(z)e^{jn\theta}$ or $e^{jz\cos\theta} = \sum_{n=-\infty}^{\infty} j^n J_n(z)e^{jn\theta}$, where $J_n(z)$ is the Bessel function of the first kind of order n. This results in $e^{-j\Omega\tau_{d,n}}$ being expressed as $2N_b + 2N_h$ nested summations whose inside expression has the form of an exponential weighted by the product of all the Bessel functions and a power of the imaginary unit j. Plugging this result into $H(f) = \sum_{n=-\infty}^{\infty} e^{-j\Omega nT_r} e^{-j\Omega\tau_{d,n}}$, we apply $\sum_{n=-\infty}^{\infty} e^{-j2\pi fnT} = \frac{1}{T}\sum_{m=-\infty}^{\infty} \delta\left(f - \frac{m}{T}\right)$ to the resulting power series, using $f_r = 1/T_r$. $H(f)$ becomes the sum of weighted Diract delta functions located at various integer linear combinations of f_r, f_b and f_h. Using the identity $J_{-n}(x) = (-1)^n J_n(x)$ for $n \in Z$ and including $e^{-j2\pi A_0 f}$, we obtain Eq. (2). ■

Several observations can be made. First, the spectral component locations, represented by $f_{\mathbf{z}}$, are multiples of RR, multiples of HR, multiples of the burst repetition frequency, and their intermods $kf_b + lf_h + if_r$, where k, l, i are integers. Second, the coefficients are expressed in closed-form. Third, the coefficients (i.e., peak heights) are functions of f_b, f_h, f_r and the Fourier series coefficients in the delay model (1). This allows investigation into how breathing and heart patterns of movement impact the shape of the IR-UWB received spectrum.

Extension of this model to the case of general periodic transmit waveform transmitted is straightforward. Let $p(t)$ be the transmit UWB burst shape and $P(f)$ be its CTFT [2]. The radar received signal is $y(t) = p(t) * h(t)$ and its CTFT is $Y(f) = P(f)H(f)$. It follows that $Y(f)$ is equal to the right hand side of (2) after replacing $c(f_{\mathbf{z}})$ with $g(f_{\mathbf{z}}) = c(f_{\mathbf{z}})P(f_{\mathbf{z}})$. For the case of a finite observation window $w(t)$, extension is also straightforward. The channel response to a periodic train of impulses is $\tilde{h}(t) = h(t)w(t)$. Its CTFT is $\tilde{H}(f) = H(f) * W(f)$ and is equal to the right hand side of (2) after replacing "δ" with "W", where $W(f)$ is the CTFT of $w(t)$. Similarly, the channel response to a periodic train of UWB bursts with a finite observation window length is expressed as $\tilde{y}(t) = y(t)w(t)$, and its CTFT is $\tilde{Y}(f) = Y(f) * W(f)$, where $\tilde{Y}(f)$ is equal to the right hand side of (2) after replacing "δ" with "W" and "$c(f_{\mathbf{z}})$" with "$g(f_{\mathbf{z}})$" $= c(f_{\mathbf{z}})P(f_{\mathbf{z}})$.

This spectrum model, derived for a single-tap channel model with unity gain, can be easily extended to the case of a multi-tap channel model with arbitrary time-varying gains by using the principle of superposition. Such an extended model could be applied to a multi-layer model of the human thorax.

[2] $p(t)$ can be just a pulse, as it was in [5]–[7]

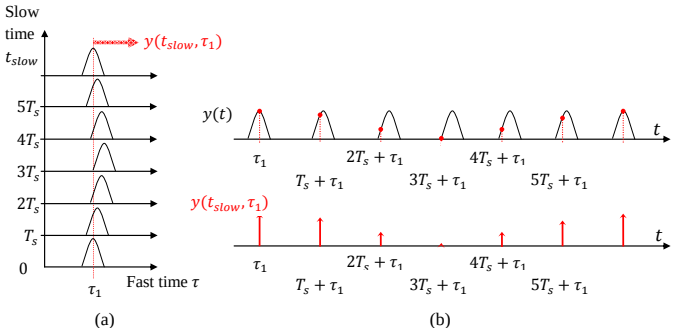

Fig. 3. Illustration of (a) the signal analyzed in [5]–[7] in the (slow time, fast time) coordinate system and (b) how it is related to the whole radar received signal on the 1D time axis. $y(t_{slow}, \tau)$ for a given τ is the signal whose CTFT is computed in [5]–[7].

IV. Further Comparison to the Models [5]–[7]

Figure 3 illustrates the aliased model used in [5]–[7]. The waveforms after static clutter removal are plotted in the slow time, fast time coordinate system in Fig. 3a. The slow time axis indicates instants when a waveform is recorded, and fast time resolves waveform features within a pulse repetition period. The samples at a given value τ_1 of fast time in the waveforms form the signal whose spectrum is analyzed in [5]–[7]. By unifying the slow time and fast time into the actual one-dimensional time, as in the two plots of Fig. 3b, it can be seen that this signal is obtained by sampling the radar received signal every T_s with some sampling offset τ_1 in the order of the pulse width. Specifically, the sampling instants are $\tau_1, T_s + \tau_1, 2T_s + \tau_1, \ldots$ (τ_1 should be thought as "fixed" in this context). This is an act of undersampling since the sampling rate is at most equal to the pulse repetition frequency f_r which is smaller than the Nyquist rate (Although not mentioned in these papers, T_s must be an integer multiple of the pulse repetition frequency, T_r.). Thus, aliasing occurs and generally we cannot use the spectrum expression in [5], [6] or [7] to synthesize the spectrum of the pre-sampling radar received signal.

Several other features differentiate our work from [5]–[7]. The spectral coefficients in our model are expressed in closed-form, whereas the spectral coefficients are provided in the form of an *integral* of the product of the CTFT of the pulse shape and one [5], two [6], or three [7] Bessel functions, or even more for a higher number of sinusoids in the pulse delay model, which does not have closed form. Another differentiation is that for a given pulse shape, the spectral coefficients $g(f_{\mathbf{z}})$ in our model are functions of the rates f_b, f_h, and f_r whereas those in the model of [6] - Eq. (15) do not.

V. Conclusion

We have developed an un-aliased model for the spectral characteristics of the IR-UWB radar received signal for an arbitrary periodic planar chest displacement model that is a sum of periodic breathing-induced and heartbeat-induced chest displacements. No assumption on the phase of these periodic displacements has been made. Closed-form representation of both the amplitude and frequency of each spectral component is provided. Although the analysis is done assuming only a planar air-skin interface, extension to multi-layered planar thorax model is straightforward by the principle of superposition. Differentiations between our model and existing models have been clarified with the focus on aliasing analysis.

Acknowledgment

This work was supported in part by Sensiotec Inc.

Dr. Mary Ann Weitnauer has a financial interest in Sensiotec Inc. which manufactures a non-contact vital signs monitor based on the IR-UWB radar technology. There is a conflict of interest management plan in place.

References

[1] E. M. Staderini, "UWB radars in medicine," *IEEE Aerospace and Electronic Systems Magazine*, vol. 17, no. 1, pp. 13–18, 2002.

[2] J. C. Lai *et al.*, "Wireless sensing of human respiratory parameters by low-power Ultrawideband impulse radio radar," *IEEE Trans. on Instrumentation and Measurement*, vol. 60, no. 3, pp. 928–938, 2011.

[3] V. Nguyen, A. Q. Javaid, and M. A. Weitnauer, "Harmonic Path (HAPA) algorithm for non-contact vital signs monitoring with IR-UWB radar," in *IEEE Biomedical Circuits and Systems Conference (BioCAS)*, 2013, pp. 146–149.

[4] ——, "Spectrum-averaged Harmonic Path (SHAPA) algorithm for non-contact vital sign monitoring with ultra-wideband (UWB) radar," in *IEEE Int. Conf. Eng. Medicine and Biology Society (EMBC)*, 2014, pp. 2241–2244.

[5] S. Venkatesh *et al.*, "Implementation and analysis of respiration-rate estimation using impulse-based UWB," in *IEEE Mil. Comm. Conf.*, 2005, pp. 3314–3320.

[6] A. Lazaro, D. Girbau, and R. Villarino, "Analysis of vital signs monitoring using an IR-UWB radar," *Progress In Electromagnetics Research*, vol. 100, pp. 265–284, 2010.

[7] M. Mabrouk *et al.*, "Model of human breathing reflected signal received by PN-UWB radar," in *IEEE Int. Conf. Eng. Medicine and Biology Society (EMBC)*, 2014, pp. 4559–4562.

[8] FCC, "Revision of part 15 of the commissions rules regarding Ultra-wideband transmission systems, first report and order," *ET Docket*, pp. 98–153, 2002.

[9] G. Varotto and E. M. Staderini, "On the UWB medical radars working principles," *International Journal of Ultra Wideband Communications and Systems*, vol. 2, no. 2, pp. 83–93, 2011.

[10] E. M. Staderini and G. Varotto, "Optimization criteria in the design of medical UWB radars in compliance with the regulatory masks," in *IEEE Biomed. Circ. Sys. Conf. (BioCAS)*, 2007, pp. 53–58.

[11] A. E. Lujan, J. M. Balter, and R. K. Ten Haken, "A method for incorporating organ motion due to breathing into 3D dose calculations in the liver: sensitivity to variations in motion," *Medical physics*, vol. 30, no. 10, pp. 2643–2649, 2003.

[12] C.-H. Hsieh, Y.-H. Shen, Y.-F. Chiu, T.-S. Chu, and Y.-H. Huang, "Human respiratory feature extraction on an UWB radar signal processing platform," in *IEEE Int. Symposium on Circuits and Systems (ISCAS)*,, 2013, pp. 1079–1082.

[13] P. S. Luna-Lozano and C. Alvarado-Serrano, "Time and amplitude relationships of the ballistocardiogram in vertical and horizontal direction." in *CCE*, 2012, pp. 1–6.

[14] W. B. Thompson, M. B. Rappaport, and H. B. Sprague, "Ballistocardiography ii. the normal ballistocardiogram," *Circulation*, vol. 7, no. 3, pp. 321–328, 1953.

[15] A. V. Oppenheim and R. W. Schafer, *Discrete-time signal processing*. Pearson, 2010.